Shape deformation and fission route of the lipid domain in a multicomponent vesicle

Kai Yang, Xi Shao, and Yu-qiang Ma*
National Laboratory of Solid State Microstructures, Nanjing University, Nanjing 210093, China
(Received 17 December 2008; revised manuscript received 16 March 2009; published 29 May 2009)

In this paper, the curvature changes and fission routes of the lipid domains in a multicomponent vesicle are studied by dissipative particle dynamics. Under different conditions of asymmetric distribution of lipids in two leaflets of lipid bilayer and area-to-volume ratio of the vesicle, we obtained different configurations of the domain in the vesicle: three typical curvature characters of the lipid domain, namely, positive, negative, and invariable curvatures compared to the vesicle are observed. Furthermore, some other morphologies of the domain and two vesicle fission routes (i.e., exocytic and endocytic fissions) are also obtained in our simulations. Particular emphasis is put on the formation of the negative curvature domain and on the behavior of endocytic fission. Based on our simulations, it is indicated that water plays an important role in the invagination and endocytic fission processes of the domain in a vesicle. For endocytic fission, domains of different sizes are evolved according to different routes under the effect of the water. Additionally, we find that both the spontaneous curvature of lipid molecules and area-to-volume ratio can promote or restrain the shape deformation of the lipid domain. Under the competition of these two factors, another possible route of endocytic fission is observed in our simulations, in that only a part of the lipid domain invaginates into the interior of the vesicle to complete the endocytic fission. Our study is helpful for understanding the possible mechanism of the shape transformation of the cellular membrane and the difference of several kinds of routes of vesicle fission.

DOI: 10.1103/PhysRevE.79.051924 PACS number(s): 87.16.−b

I. INTRODUCTION

Cells or cell organelles are surrounded by cellular membrane. The main ingredients of the membrane include phospholipids, proteins, and cholesterols [1]. One of the most important characters of cellular membrane is the heterogeneity. Different kinds of lipids distribute unevenly in the membrane and organize into complexes and domains, the so-called rafts [2,3]. The heterogeneity has been observed in experiments, for example, the sphingolipids with saturated acyl tail chains can form the liquid-ordered (l_o) domains with cholesterol, whereas the phospholipids with unsaturated acyl chains can form liquid-disordered (l_d) domains in model membranes [4]. Another essential character of cellular membrane is its curvature or shape character. It has been experimentally found that the membrane can be transformed into a fascinating variety of shapes, such as sphere, tube, and discocyte [5].

It is generally believed that many important biological phenomena in cells are associated with both the heterogeneity and curvature characters of cellular membrane [6–8]. The typical examples are the budding and fission of cellular membrane. In experiments, the protrusive lipid domains and exocytic fission behaviors have been observed in the lipid giant unilamellar vesicles (GUVs) or liposomes. These phenomena are related to the lipid structure, distribution, external environment stimulus, and so forth [9,10]. Moreover, the striking shape deformation of the domain and fission behaviors of GUVs is found in recent experiments. Bacia *et al.* [11] observed the negative curvature l_0 domain and a new type of budding manner, "budding in," in GUVs with the application of confocal fluorescence microscopy and fluorescence correlation spectroscopy. They speculated that the molecular structure of the sterols and their location in lipid bilayer are the possible reasons. Hamada and co-workers [12] also observed the invagination of lipid raft and endocytic fission in giant liposome with the addition of Triton X-100. Two endocytic fission routes of lipid rafts with different sizes are found in their experiments. In addition, the change in lipid molecular structure can also trigger the negative curvature domain and endocytic fission [13,14]. These experimental results clearly indicate that lipid bilayer can deform itself in different directions and adopt various fission routes under different conditions. However, the mechanism of the control of shape deformation of cellular membrane and the difference between various fission routes are still largely unknown. To explore how membrane regulates its curvature or fission route is significant to deeply understand the function of the cell and has possible biomedical applications. For example, endocytose and exocytose are two main pathways of intracellular trafficking [1]. Additionally, some pathogenesis, such as atherosclerosis, Parkinson, and Alzheimer, may be associated with special curvature changes of lipid rafts [13]. Due to the restriction of instruments, it is very difficult for experiments to solely reveal the underlying mechanism, and thus theoretical studies become necessary. Furthermore, although exocytic fission behaviors of the vesicle have been studied before [15–17], a few computer simulations have been carried out to systematically examine the direction of shape deformation of the lipid domain and the behavior of endocytic fission of the vesicle.

To examine the dynamics of budding and fission in multicomponent lipid bilayer, computer simulation is a powerful tool. It can include the molecular details of lipids which are ignorable by the continuum model [18]. Molecular-dynamics (MD) simulations have offered us more insights into the cellular membranes [19]. Nevertheless, small system size and

*Author to whom correspondence should be addressed; myqiang@nju.edu.cn

time scale are restricted in MD. To overcome these problems, coarse-gained (CG) simulation methods have been employed [15,20,21]. Dissipative particle dynamics (DPD) is an effective coarse-gained simulation method and has been extensively employed in cellular membrane systems [16,17,22–26]. DPD is a mesoscopic simulation technique with hydrodynamic interaction. Each DPD particle is composed of a group of atoms or molecules. The soft interaction between DPD particles allows a larger simulation time step and space scale. Recent studies have shown that DPD simulation could reproduce proper characters of lipid bilayer, such as density distribution and surface stress profile, and could mimic some important dynamic behaviors of the membrane [16,22,25,27].

In this paper, we study different shape changes and fission routes of the domain in the multicomponent lipid vesicle, especially the formation of negative curvature domains and behaviors of endocytic fission, using dissipative particle dynamics method. The vesicle is composed of three kinds of lipids. Those lipids in the domain are distributed asymmetrically in two leaflets of the bilayer. The radii of their head beads can be changed. The effects of the asymmetry distribution of lipids, the area-to-volume ratio of the vesicle, the domain size, and the spontaneous curvature of the lipids on the evolution of the domain in the vesicle are examined. The interplay among these effects results in different deformation directions, curvature characters, and fission routes of the lipid domain. In particular, the formation of negative curvature domain and the dynamics of endocytic fission are investigated in detail. In addition, it is worth to note that due to the constraint of computer power, the size of our vesicle, which is similar to that of vesicles adopted in other simulations about fission behaviors [15–17,28], is much smaller than GUVS. Thus, a direct comparison between our simulations and experiments is difficult. However, we believe that our results will be helpful to qualitatively understand the mechanism of the regulation of shape deformation direction, the features of various fission routes, and the possible influential factors.

This paper is organized as follows. In Sec. II DPD simulation model and technique are presented. In Sec. III the simulation results and discussion are described. Finally, our conclusion is given in Sec. IV

II. MODEL AND SIMULATION METHOD

A. DPD model for lipids and water

In our simulation, the lipid molecule is modeled as a linear chain with two hydrophilic head beads (H) and five hydrophobic tail beads (T). These beads are connected by the harmonic springs. There are three kinds of lipids (denoted as A, $B1$, and $B2$) in our simulation. The introduction of B-type lipids ($B1$ and $B2$) is to form a domain in the matrix of lipid A, so they are chosen to segregate from lipid A. All tail beads of three kinds of lipids and the head beads of A-type lipids have the same radius (R_0), whereas the radii of head beads of lipids $B1$ and $B2$ can be changed within a certain range (0.8–1.2 units of R_0). The only difference between lipids $B1$ and $B2$ is that their head beads radii may be different. Additionally, water is explicitly included in the simulation system. One water bead (S) roughly includes three water molecules. It has the same mass (m_0) and radius (R_0) as the head bead of the A-type lipid, and these set the mass and length scale in the simulation. Also, the time scale in the simulation can be derived from the dynamics (e.g., diffusion) processes of the water beads [27,29].

B. DPD simulation method

Dissipative particle dynamics is first introduced by Hoogerbrugge and Koelman to describe the mesoscopic hydrodynamic behaviors of complex fluids and later improved by Espagnol and Warren [30,31]. In our simulations, we adopt a modified DPD method, in which the radius R and mass m of a single DPD bead can vary [24,29]. The evolution of the position and velocity of DPD bead i, $(\mathbf{r}_i, \mathbf{v}_i)$, obeys Newton's equation of motion,

$$\frac{d\mathbf{r}_i}{dt} = \mathbf{v}_i, \quad \frac{d\mathbf{v}_i}{dt} = \frac{\mathbf{f}_i}{m}, \tag{1}$$

where $m/m_0 \propto R^3$.

The force $\mathbf{f}_i$ of bead i includes three types of forces:

$$\mathbf{f}_i = \sum_{j \neq i} (\mathbf{F}_{ij}^C + \mathbf{F}_{ij}^D + \mathbf{F}_{ij}^R). \tag{2}$$

The conservative force $\mathbf{F}_{ij}^C$ between beads i and j is

$$\mathbf{F}_{ij}^C = \begin{cases} a_{ij}\left(1 - \frac{r_{ij}}{r_c}\right)\hat{\mathbf{e}}_{ij}, & r_{ij} < r_c \\ \mathbf{0}, & r_{ij} \geq r_c, \end{cases} \tag{3}$$

where $r_{ij} = \mathbf{r}_i - \mathbf{r}_j$, $\hat{\mathbf{e}}_{ij} = \frac{\mathbf{r}_{ij}}{r_{ij}}$. The parameter r_c is the cutoff radius of the conservative force, defined as $r_c = \frac{1}{2}(R_i + R_j)$, where R_i and R_j are the radii of beads i and j, respectively. a_{ij} is the maximum repulsion interaction between beads i and j.

The dissipative force $\mathbf{F}_{ij}^D$ is

$$\mathbf{F}_{ij}^D = \begin{cases} -\gamma_{ij}\left(1 - \frac{r_{ij}}{r_c}\right)^2 (\hat{\mathbf{e}}_{ij} \cdot \mathbf{v}_{ij})\hat{\mathbf{e}}_{ij}, & r_{ij} < r_c \\ \mathbf{0}, & r_{ij} \geq r_c, \end{cases} \tag{4}$$

where $\mathbf{v}_{ij} = \mathbf{v}_i - \mathbf{v}_j$. γ_{ij} is the strength of friction between beads i and j.

Finally, the random force $\mathbf{F}_{ij}^R$ takes the form as

$$\mathbf{F}_{ij}^R = \begin{cases} \sqrt{2\gamma_{ij}k_BT}\left(1 - \frac{r_{ij}}{r_c}\right)\zeta_{ij}\hat{\mathbf{e}}_{ij}, & r_{ij} < r_c \\ \mathbf{0}, & r_{ij} \geq r_c, \end{cases} \tag{5}$$

where ζ_{ij} is a symmetric random variable with zero mean and unit variance, i.e., $\langle \zeta_{ij}(t) \rangle = 0$ and $\langle \zeta_{ij}(t)\zeta_{i'j'}(t') \rangle = (\delta_{ii'}\delta_{jj'} + \delta_{ij'}\delta_{ji'})\delta(t-t')$.

In order to ensure the integrality of lipids, the harmonic spring interaction is applied between neighboring beads in a single molecule as follows:

$$\mathbf{F}_s = -k_s\left(1 - \frac{r_{i,i+1}}{l_0}\right)\hat{\mathbf{e}}_{i,i+1}, \tag{6}$$

where l_0 is the equilibrium bond length and k_s is the spring constant. The rigidity of lipid tails is denoted by a three-body potential U_b [22],

$$U_b = k_b[1 - \cos(\varphi - \varphi_0)], \tag{7}$$

where k_b is the constant; φ is the bond angle of the two bonds connecting three beads $i-1$, i and $i+1$; and φ_0 is the preferred angle.

Our simulations apply DPD velocity-Verlet integration algorithm [32] with the iteration time step $\Delta t=0.02\tau$ ($\tau=[m_0R_0^2/(k_BT)]^{1/2}$ is the unit of simulation time). For simplicity, all the physical quantities are in units of the bead radius R_0, mass m_0, and temperature k_BT.

C. Simulation conditions and parameters

All simulations are performed in the *NVT* ensembles at the temperature $k_BT=1$. The size of simulation box is $42\times42\times42$ with the number density $\rho=3$. There are a total of 222 264 DPD beads in the simulation box, and the periodic boundary conditions are adopted in three directions.

The character of beads, hydrophobicity or hydrophilicity, determines the value of the repulsion interaction a_{ij}. The value of a_{ij} is set to $a_{ij}=25$ between the same type of beads and $a_{ij}=95$ between the different types of beads. Additionally, for lipids, we set the equilibrium bond length $l_0=0.5$ and $k_s=128$. The chain rigidity constant is set to $k_b=5$ and $\varphi_0=0$. These values could well produce the structure and mechanical character of lipid bilayers [29]. To realize the phase separation of lipids A and $B1$ (or $B2$), we set the parameters $a_{HA,HB1(2)}=40$ and $a_{TA,TB1(2)}=40$. There is no difference in describing the interaction between lipids $B1$ (or $B2$) and other components. The detailed value of a_{ij} is given by

$$\mathbf{a}_{ij} = \begin{pmatrix} & S & H_A & T_A & H_{B1(2)} & T_{B1(2)} \\ S & 25 & 25 & 95 & 25 & 95 \\ H_A & 25 & 25 & 95 & 40 & 95 \\ T_A & 95 & 95 & 25 & 95 & 40 \\ H_{B1(2)} & 25 & 40 & 95 & 25 & 95 \\ T_{B1(2)} & 95 & 95 & 40 & 95 & 25 \end{pmatrix}.$$

The vesicle used in our simulations is prepared by randomly distributing 4200 lipids A in the inner and outer leaflets of a nearly closed spherical surface [16]. In order to ensure the vesicle near zero surface tension, we open two holes in the top and bottom of the vesicle initially, and then 50 000 simulation iterations are carried out to close the two holes and equilibrate the system. After equilibrium, the vesicle is closed and nearly spherical [Fig. 1(a)]. The ratio of the number of lipids between the inner and the outer leaflets of bilayer is approximately 0.6, and there are about 12 094 water beads in the interior of the vesicle. The vesicle with different area-to-volume ratios can be realized by removing some water beads from the interior of the vesicle. Here, the area-to-volume ratio Π is defined as the ratio of the number of total lipids beads to the total beads inside the vesicle. Due to the relatively long tail adopted in the coarse-grained model of the lipid molecules and their strong hydrophobic character, the water cannot pass through the vesicle or the domain in our simulations. Therefore, the area-to-volume ratio can be effectively controlled by this way. The formation of the domain is possible to be realized by quenching the multicomponent vesicle into two-phase regions from a higher temperature. But the completely coarsening of small domains in the vesicle is rather time consuming [16,33,34], and then this will make it difficult to quantitatively investigate the influence of the domain size and the lipid composition in two leaflets of the domain. Therefore, we prepare the domain by replacing some lipid A at the top of vesicle with lipids $B1$ and $B2$ [15,28] [Fig. 1(b)]. The flip-flop of the lipid can occur in the cellular membrane but it is an extremely slow process [35]. In our simulations, the amount of flip-flop of lipids is rather small (less than 1% of the lipids in the domain) and its occurrence is sporadic. Therefore, the effect of the flip-flop can be neglected in our simulations, and we always assume that lipids $B1$ and $B2$ are located in the inner and outer leaflets of the vesicle, respectively.

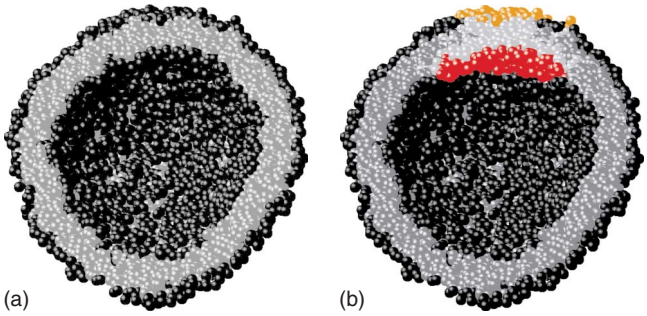

FIG. 1. (Color online) Cross-section image of initial configuration of (a) vesicle and (b) domain. Here, water molecules are not displayed. The vesicle in (a) and the major of the vesicle in (b) are composed of lipid A. The domain in the top of the vesicle in (b) is composed of lipids $B1$ and $B2$. Black: head beads of lipid A; gray: tail beads of lipid A; red: head beads of lipid $B1$ (in the lower part of the domain); orange: head beads of lipid $B2$ (in the upper part of the domain); light gray: tail beads of lipids $B1$ and $B2$.

The main variables of our simulation are (1) the radii of head beads of lipids $B1$ and $B2$, R_{B1} and R_{B2}, that can infer the effect of the spontaneous curvature of the lipid molecule; (2) the area-to-volume ratio Π of the vesicle; and (3) the fraction of lipids $B1$ and $B2$, $\Phi_{B1}=N_{B1}/N$ and $\Phi_{B2}=N_{B2}/N$, where N_{B1}, N_{B2}, and N are the numbers of lipid $B1$, lipid $B2$, and total lipids in the simulation box, respectively. Also, we denote the fraction Φ_B of B-type lipids as $\Phi_B=\Phi_{B1}+\Phi_{B2}$ which can reflect the domain size.

III. RESULTS AND DISCUSSION

A. Effect of the asymmetric distribution of lipids

In cellular membranes, lipids are always distributed asymmetrically in two leaflets of the bilayer. For example, phosphatidylserine and phosphatidyletholamine are predominantly in the cytosolic leaflet, whereas most

FIG. 2. (Color online) Three typical curvature characters of the domains in the multicomponent vesicle (cross section). (a) Positive curvature: $\Phi_{B1}/\Phi_{B2}=1/3.75$, $\Phi_B=6.7\%$, and $\Pi=0.73$; (b) invariable curvature: $\Phi_{B1}/\Phi_{B2}=1/1.6$, $\Phi_B=6.7\%$, and $\Pi=0.73$; (c) negative curvature: $\Phi_{B1}/\Phi_{B2}=3/1$, $\Phi_B=6.7\%$, and $\Pi=0.73$. $R_{B1}=1.0$ unit of R_0 and $R_{B2}=1.0$ unit of R_0.

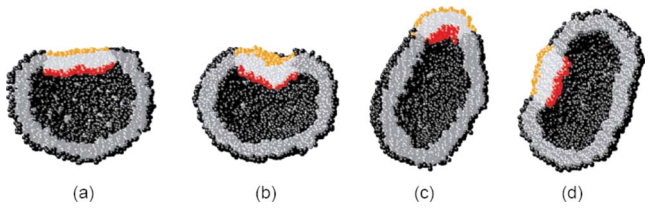

FIG. 3. (Color online) Some curvature characters of the domains in the multicomponent vesicle (cross section). (a) Negative curvature (plane): $\Phi_{B1}/\Phi_{B2}=2/1$, $\Phi_B=6.7\%$, and $\Pi=0.73$; (b) negative curvature (wrinkle): $\Phi_{B1}/\Phi_{B2}=2/1$, $\Phi_B=6.7\%$, and $\Pi=0.75$; (c) ellipsoidal curvature I: $\Phi_{B1}/\Phi_{B2}=1/2$, $\Phi_B=6.7\%$, and $\Pi=0.78$; (d) ellipsoidal curvature II: $\Phi_{B1}/\Phi_{B2}=1.2/1$, $\Phi_B=6.7\%$, and $\Pi=0.78$. $R_{B1}=1.0$ unit of R_0 and $R_{B2}=1.0$ unit of R_0.

phosphatidylcholine and sphingomyeline are located in the outer leaflet of the plasma membrane of eukaryotic cells [36]. The asymmetrical distribution of lipids has important influence on the shape deformation of cellular membranes. Experimentally, Inaoka *et al.* [37] found that the difference of the distribution of amphiphiles in two leaflets of the bilayer can result in the vesiculation transition and fission of the giant unilamellar vesicles. Theoretically, the area difference elasticity (ADE) theory concludes that the area difference effect can create effective nonlocal curvature energy, leading to the shape transformation of lipid bilayers [5,38,39]. According to the ADE theory, the equilibrium shape of a membrane with area (A) is obtained by optimizing the free energy (F_{ADE}), which could be taken as [5]

$$F_{\mathrm{ADE}}=\kappa\left[\frac{1}{2}\oint dA(2H)^2+\frac{\alpha\pi}{2Al^2}(\Delta A-\Delta A_0)^2\right], \qquad (8)$$

where κ is the bending rigidity, H is the mean curvature, l is the distance between two leaflets of the bilayer, and α is the numerical constant. The first term of the equation is the bending energy of the membrane and the second term represents the energy induced by the deviation of the total area difference ΔA from ΔA_0. ΔA_0 in the second term is the intrinsic area difference of the membrane, which is defined as $\Delta A_0=(N_{out}-N_{in})a_0$, where a_0 is the cross section of a lipid and N_{out} and N_{in} are the numbers of lipids in outer and inner leaflets of lipid bilayer, respectively. From Eq. (8), it is found that ADE effect can be realized in the simulations by the difference in the number of lipids in two leaflets of the bilayer.

Under the effect of the asymmetric distribution of lipids (Φ_{B1}/Φ_{B2}) and area-to-volume ratio (Π), the domains in the vesicle will be deformed into different configurations, which are summarized in Fig. 5. When the area-to-volume ratio is small ($\Pi<0.75$); the excess area of the vesicle becomes also small. The parent vesicle keeps basically spherical and the deformation of the domains is mostly regulated by the ratio of lipids $B1$ and $B2$ (Φ_{B1}/Φ_{B2}). If Φ_{B1}/Φ_{B2} is equal or very close to the ratio of the number of lipids in the two leaflets of the parent vesicle, the curvature of the domain keeps unchanged compared to the parent vesicle [invariable curvature, Fig. 2(b), and the region occupied by cyan circle in Fig. 5]. This corresponds to the case of $\Delta A=\Delta A_0$ in the ADE free-energy expression and we call $\Phi_{B1}/\Phi_{B2}=1/1.6$ as "matching point." When Φ_{B1}/Φ_{B2} is much less ($\Phi_{B1}/\Phi_{B2}=1/3.75$ or 1/3) or larger ($\Phi_{B1}/\Phi_{B2}=3/1$) than this point, the domain will protrude outward [positive curvature, Fig. 2(a), and the region occupied by pink star in Fig. 5] or invaginate inward to form the bowl-like shape [negative curvature, Fig. 2(c)]. In these cases, the curvature change of the domain with Φ_{B1}/Φ_{B2} is in agreement with the ADE theory well. Additionally, our results are also qualitatively consistent with the model of Taniguchi [34], which supplies numerical evidences that asymmetric distribution of lipids in two leaflets of lipid bilayer can effectively change the shape of the bilayer. Notice that the curvature change of the domain depends on the size of the vesicle. For the vesicle of different sizes, the number of lipids located in two leaflets of the bilayer is different. Therefore, to produce the same curvature domain, different values of Φ_{B1}/Φ_{B2} are required for different vesicles. In addition, besides three typical curvature characters, there are still other configurations of the domain observed in our simulations. For example, there are two kinds of new negative curvature domains [Figs. 3(a) and 3(b)]. Based on the ADE model, when $\Phi_{B1}/\Phi_{B2}>1$ the domain would invaginate inward to form a bowl-like shape. However, as shown in Figs. 3(a) and 3(b), for the domain whose Φ_{B1}/Φ_{B2} is slightly more than 1 ($\Phi_{B1}/\Phi_{B2}=1.2/1$ or 2/1), domain is planar or wrinkled. Similar configuration of the domain is also observed when Π takes the smallest value ($\Pi=0.71$) but Φ_{B1}/Φ_{B2} is large ($\Phi_{B1}/\Phi_{B2}=3/1$). The appearance of these morphologies may be caused by the explicit incorporation of the molecular structure of the lipids and water in our simulations. Because the value of Φ_{B1}/Φ_{B2} of these domains is not very large, the corresponding ADE energy is small. On the other hand, for small Π, there is still much water molecules inside the vesicle. Thus the invagination of the domain will be blocked greatly by the existence of water. The bending of lipid molecules or the bilayer becomes a possible way to release the strain caused by the local asymmetrical distribution of the lipids in two leaflets. On the contrary, the domains with the bowl-like negative curvatures occur mainly when Φ_{B1}/Φ_{B2} is enough large and Π is not very small (e.g., $\Phi_{B1}/\Phi_{B2}=3/1$ and $\Pi=0.73$; $\Phi_{B1}/\Phi_{B2}=2/1$ and $\Pi=0.78$). Additionally, all these domains evidently invaginate inward compared to the parent vesicle. So, for the sake

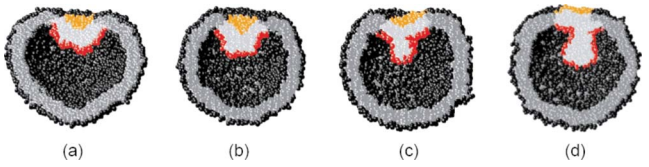

FIG. 4. (Color online) Collapse of inner leaflet of the domains in the multicomponent vesicle. The cross-section images are taken at times (a) 70, (b) 100, (c) 300, (d) 1000 units of τ, respectively. $\Phi_{B1}/\Phi_{B2}=3/1$, $\Phi_B=6.7\%$, and $\Pi=0.75$. $R_{B1}=1.0$ unit of R_0 and $R_{B2}=1.0$ unit of R_0.

of simplicity, in Fig. 5, we do not distinguish these negative curvatures (the region occupied by purple square in Fig. 5).

With the increase in the area-to-volume ratio ($\Pi>0.75$), shape deformations of the domains become more complicated and some cases are also beyond the scope of the analytical continuous theory. When Φ_{B1}/Φ_{B2} is enough small ($\Phi_{B1}/\Phi_{B2}=1/3.75$ or $1/3$) or much large ($\Phi_{B1}/\Phi_{B2}=3/1$), the domain can be deformed very strongly because of the strong area different effect. Thus fission is observed (the region occupied by red inverse or green triangle in Fig. 5). For the occurrence of exocytic fission, Φ_{B1}/Φ_{B2} should be smaller than 1/2.4 and for the occurrence of endocytic fission, Φ_{B1}/Φ_{B2} should be larger than 2.5/1 when $\Pi=0.78$. Therefore, for any domain whose Φ_{B1}/Φ_{B2} is between two thresholds, it will stay in parent vesicle. However, it is observed in our simulations that the shape deformation of the domain is completely different from the corresponding case with the small area-to-volume ratio. Due to the large area-to-volume ratio, the shape of the parent vesicle will be transformed into an ellipsoidlike one. So the domain will be "moved" to the region of the parent vesicle that closely matches its spontaneous curvature, rather than protrude outward or invaginate inward as before [Figs. 3(c) and 3(d)]. Also, for simplicity, in Fig. 5, all similar cases are represented as "ellipsoidal" curvatures (the region occupied by blue diamond in Fig. 5). In addition, when the value of the area-to-volume ratio is in the middle range (for example, Π is equal or close to 0.75) but Φ_{B1}/Φ_{B2} is enough large ($\Phi_{B1}/\Phi_{B2}=3/1$), a different configuration of the domain, "monolayer collapse," is observed in our simulations [Fig. 4(d) and the region occupied by orange plus in Fig. 5]. Under these simulation conditions, the domain tends to strongly invaginate inward. But there is no enough excess area and interior space of the vesicle for the deformation of the domain due to the relatively small area-to-volume ratio. Therefore, the domain buckles initially and then only lipids in the inner leaflet collapse (Fig. 4). The appearance of this configuration is also supposed to be related to the incorporation of the molecular structure of the lipid in the simulations, rather than regarding the bilayer as an infinitely thin sheet, as is usually done in some phenomenological models. The similar structure has been found by Tieleman *et al.* in their molecular simulations of lipid monolayer [40]. It is noted that this configuration is observed in our simulations only when the direction of shape deformation of the domain is inward.

In addition, phase separation also plays an important role in the shape deformation and fission of the domain in the vesicle. Under different strengths of phase separation

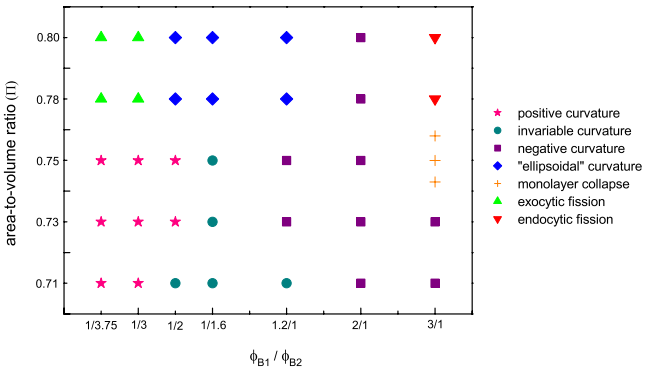

FIG. 5. (Color online) Final configurations of the domain in the vesicle with different ratios Φ_{B1}/Φ_{B2} and the area-to-volume ratio Π when $\Phi_B=6.7\%$. The results are obtained at $t=5000$ units of τ. Pink star: positive curvature; cyan circle: invariable curvature; purple square: negative curvature; blue diamond: ellipsoidal curvature; orange plus: monolayer collapse; green triangle: exocytic fission; red inverse triangle: endocytic fission.

($a_{HA,HB1(2)}$ and $a_{TA,TB1(2)}$), shape deformations and the occurrence possibilities of the fission of the domains are varied. When the strength of phase separation is sufficiently strong ($a_{HA,HB1(2)}=50$ and $a_{TA,TB1(2)}=50$), the domains always fission from the vesicle [Fig. 6(a)]. The fission route is mainly determined by the ratio Φ_{B1}/Φ_{B2}: when $\Phi_{B1}/\Phi_{B2}\leq 1/1.6$, exocytic fission occurs; when $\Phi_{B1}/\Phi_{B2}>1/1.6$, endocytic fission is possible to occur (when $\Phi_{B1}/\Phi_{B2}=3/1$ but $\Pi=0.71$ or 0.73, the domain initially invaginates inward. However, due to the small area-to-volume ratio, there is no enough space inside the vesicle to accommodate the domain. Thus domain will be "pushed" slowly outside the vesicle). When the strength of phase separation is weak ($a_{HA,HB1(2)}=30$ and $a_{TA,TB1(2)}=30$), no fission could occur in any cases [Fig. 6(b)]. The domains are only deformed with different curvatures in the vesicle.

From Figs. 5 and 6, it is indicated that with the variance of the ratio Φ_{B1}/Φ_{B2} and Π, the direction of shape deformation, and the fission route of the domain will be regulated. The asymmetrical distribution of lipids is an effective way for the shape deformation of the bilayer. Especially, for the larger Φ_{B1}/Φ_{B2}, both the negative curvature domain and some other configurations of the domain are obtained. Also, endocytic fission could be realized. Fission is a vital biological process of cellular membrane. The behavior of exocytic fission has been studied before [15–17,25]. In the following sections, we will adopt the parameters $\Phi_{B1}/\Phi_{B2}=3/1$ and $a_{HA,HB1(2)}=40$, and $a_{TA,TB1(2)}=40$ (unless special statements) and focus on the behavior of endocytic fission.

B. Effect of the domain size on endocytic fission

The evolutions of the domains of three sizes ($\Phi_B=6.7\%$, 8.5%, and 13%; $\Phi_{B1}/\Phi_{B2}=3/1$) in the vesicles are investigated in our simulations. It is found that the domains of different sizes are evolved with different fashions under the same simulation conditions. For the largest domain ($\Phi_B=13\%$), no fission is observed even after enough long simulation time. At last, it still stays in the vesicle. The main

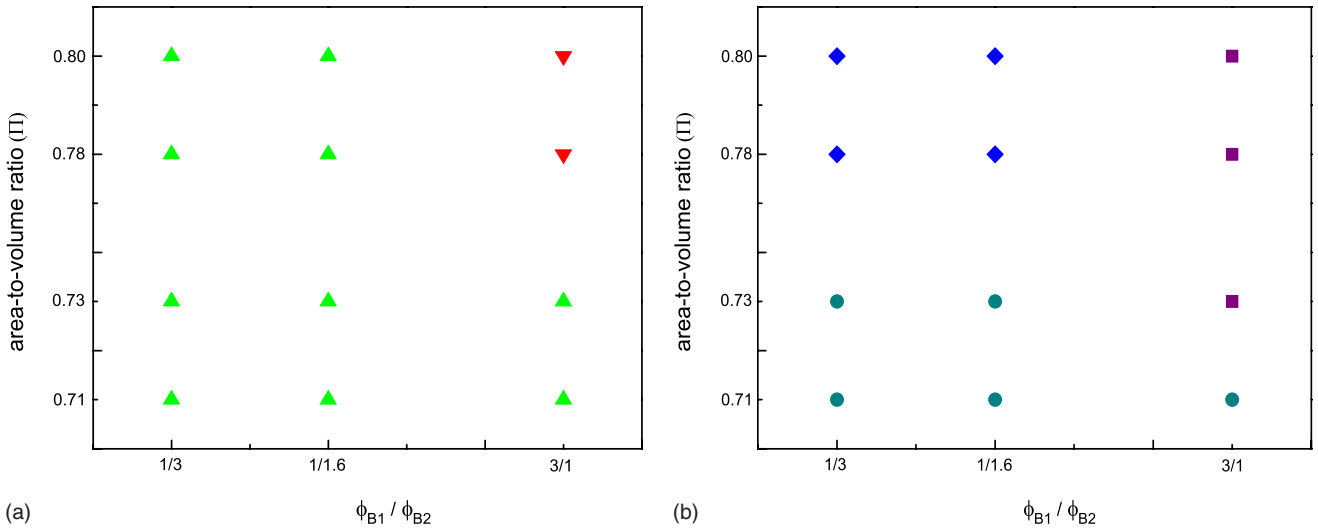

FIG. 6. (Color online) Final configurations of the domain in the vesicle with different strengths of phase separation when Φ_B=6.7%. (a) $a_{HA,HB1(2)}$=50 and $a_{TA,TB1(2)}$=50; (b) $a_{HA,HB1(2)}$=30 and $a_{TA,TB1(2)}$=30. The results are obtained at t=5000 units of τ. Cyan circle: invariable curvature; purple square: negative curvature; blue diamond: ellipsoidal curvature; green triangle: exocytic fission; red inverse triangle: endocytic fission.

change of the domain is that its curvature becomes negative in comparison with that of the vesicle. However, for the other two smaller domains (Φ_B=6.7% and 8.5%), endocytic fissions occur. Both of them invaginate inward and finally segregate from the parent vesicle and form daughter vesicles.

Even for the two smaller domains, there still exist some differences in their processes of endocytic fission. The typical time evolutions of endocytic fission of two small domains are demonstrated in Figs. 7 and 8, respectively. For the smallest domain (Φ_B=6.7%), it first bends inward [Fig. 7(a)], and then the total domain invaginates into the parent vesicle and forms a tubelike bud [Fig. 7(b)]. Afterward, the neck comes into being completely inside the parent vesicle [Figs. 7(c) and 7(d)] and finally the bud segregates from the parent vesicle and forms a daughter vesicle [Fig. 7(e)]. When the domain size becomes larger, its evolution differs somewhat. For the larger domain of size Φ_B=8.5%, its incipient shape changes are basically similar to that of the smallest domain [Figs. 8(a) and 8(b)]. But the main difference appears in the process of the neck formation. As shown in Figs. 8(c) and 8(d), the bud first becomes flask shaped and then leans to form the neck near the top of the vesicle. It is noted that there are still a certain fraction of lipid B (domain) in the parent vesicle at this time. Only after the formation of the neck the bud slowly pinches off inside the parent vesicle [Fig. 8(e)]. In experiment, Hamada and co-workers [12] also find that the manners of endocytic fission are different with the increase in lipid domain.

The interface energy U_{BA} can be calculated from the bead-bead conservative interactions between lipids A and B as

$$U_{BA} = \begin{cases} \sum \frac{1}{2} a_{ij} \left(1 - \frac{r_{ij}}{r_c}\right)^2, & r_{ij} < r_c \\ 0, & r_{ij} \geq r_c. \end{cases}$$

Its change can reflect the evolutive features of domains. Figure 9(a) shows the changes in U_{BA} of three domains. The changes in U_{BA} of the two smaller domains are similar but evidently distinguished from that of the largest domain. These are consistent well with the final configurations of three domains: the largest one keeps in the vesicle but the other two domains complete endocytic fissions. Interestingly, the time evolution of the interaction energy between the domain and water also shows similar change tendency to that of the interface energy [Fig. 9(b)].

We take the evolution of the domain of size Φ_B=6.7% as the example. The evolution of interface energy can be roughly divided into four stages (0–60τ, 60–250τ, 250–480τ, and 480–600τ) according to the slope change of the energy curve that exactly corresponds to different shape transitions of the domain (Fig. 7). The initial rapid decrease in U_{BA} is possibly caused by the strong area difference effect and finally U_{BA}=0 reveals the complete segregation of the domain from the parent vesicle. In addition, it is found from Fig. 9(a) that the decrease in U_{BA} becomes obviously slow at stages 2 and 3. The behavior of slowing down is possible to be induced by the coupling of asymmetric distribution of lipids in two leaflets to the deformation of the membrane [34]. Besides this factor, based on our simulations, water is also possible to play an important role in this behavior. From the fission process of the vesicle, we find that domain invaginates inward to form a bud in stage 2 and the neck of the bud will be formed at the end of stage 3. Also, the parent vesicle

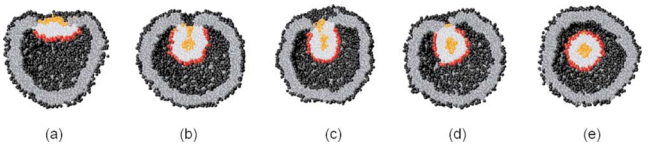

FIG. 7. (Color online) Snapshots of endocytic fission of domain of size Φ_B=6.7% (Φ_{B1}/Φ_{B2}=3/1). The cross-section images are taken at times (a) 60, (b) 250, (c) 400, (d) 480, and (e) 600 units of τ, respectively. R_{B1}=1.2 units of R_0, R_{B2}=0.8 units of R_0, and Π =0.78.

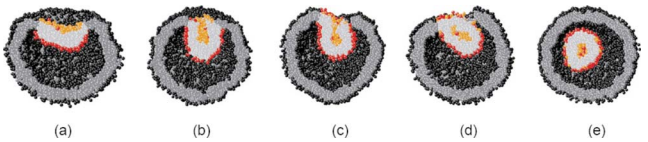

FIG. 8. (Color online) Snapshots of endocytic fission of domain of size $\Phi_B=8.5\%$ ($\Phi_{B1}/\Phi_{B2}=3/1$). The cross-section images are taken at times (a) 150, (b) 500, (c) 1,500, (d) 1,675, and (e) 3000 units of τ, respectively. $R_{B1}=1.2$ units of R_0, $R_{B2}=0.8$ units of R_0, and $\Pi=0.78$.

gradually becomes more spherical. For exocytic fission, the direction of the budding of the domain is outward and the water near the domain could be pushed away easily. However, for endocytic fission, the interior space of the vesicle is finite. With the invagination of the domain, the interior space of the vesicle for water to freely move will be reduced. Therefore, the invagination will incur the counteraction of the water inside the vesicle. Figure 9(b) shows the interaction energy between the domain and water. It is found that this energy indeed increases strongly. So it is inferred that water is important for the shape deformation and endocytic fission of the vesicle.

The whole fission process requires strong shape deformation of both the parent vesicle and the domain. For the parent vesicle, its interior space becomes more jam packed with the invagination of the domain, so the interaction energy between water and lipid A increases constantly until the neck is basically formed [Fig. 10(a), $\sim 480\tau$]. Such an increase in the interaction energy indicates that the parent vesicle becomes "tight." Hence, the deformation of the vesicle will be hindered. Furthermore, water molecules play more complex roles in the endocytic fission process of lipid domain. In general, the interaction between water and domain increases in the whole fission process [Fig. 9(b)]. However, the interactions between water and two leaflets of bilayer are different. As shown in Fig. 10(b) [the green (upper) line], the interaction energy between water and the inner leaflet of the domain (the one is close to the interior of the parent vesicle) increases with the invagination of the domain. As mentioned above, this is caused by the resistance of water inside the vesicle. This interaction tends to compress the domain and minimize the volume of the bud. On the other hand, there is still water inside the outer concave of the bud [Fig. 10(b), the red (bottom) line]. Although the number of these water beads is reduced due to the compression of the domain, their existence will also block the shape deformation of the domain. Specially, for the formation of the neck, it is also influenced by this competition. It could be realized only after the interaction energy between water and the outer leaflet of the domain reaches its minimum [Fig. 10(b), the lowest point of red (bottom) line, $\sim 440\tau$]. In addition, the formation of the neck needs the contraction of the rim of the domain. So the fission process in stage 3 will be further slowed. After the formation of the neck, the domain will segregate from the parent vesicle soon (stage 4).

On the basis of the above results, it is suggested that the water plays vitally important roles in the endocytic fission processes. Furthermore, it also offers a possible explanation to the different evolution routes of the larger domains. For the domain of size $\Phi_B=8.5\%$, because of its larger domain size, its invagination will occupy more interior space of the parent vesicle and incur the stronger resistant interaction of water [Fig. 9(b)]. Under this stronger resistant effect of the water, the bud has to lean and keep a certain fraction of lipid B in parent vesicle in order to minimize its volume inside the parent vesicle in the process of the neck formation. Furthermore, if the domain size continues to increase, it is impossible for the parent vesicle to provide enough interior space to accommodate the bud completely. Thus any further invagination of the domain will incur the strongest resistance of water [Fig. 9(b)]. Therefore, for the domain of size $\Phi_B=13\%$, it stays in the negative curvature state and no endocytic fission will occur. Conclusively, the evolution of the domain in a vesicle is rather complicated, which will be in-

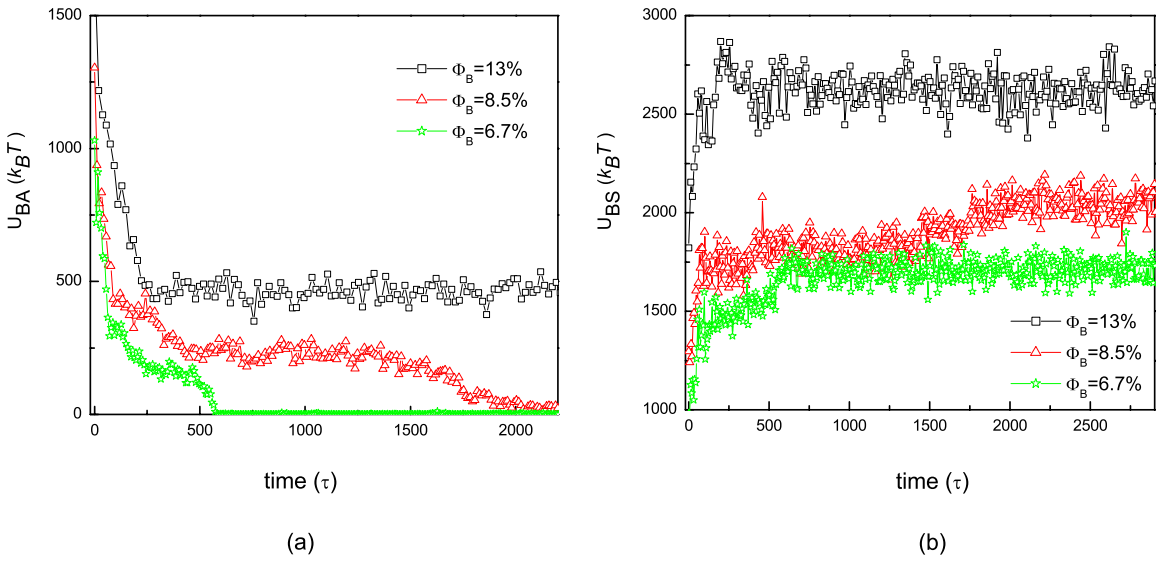

FIG. 9. (Color online) Time evolution of (a) the A-B interface energy and (b) domain-water interaction energy for different sizes of domains. $\Phi_{B1}/\Phi_{B2}=3/1$, $R_{B1}=1.2$ units of R_0, $R_{B2}=0.8$ units of R_0, and $\Pi=0.78$.

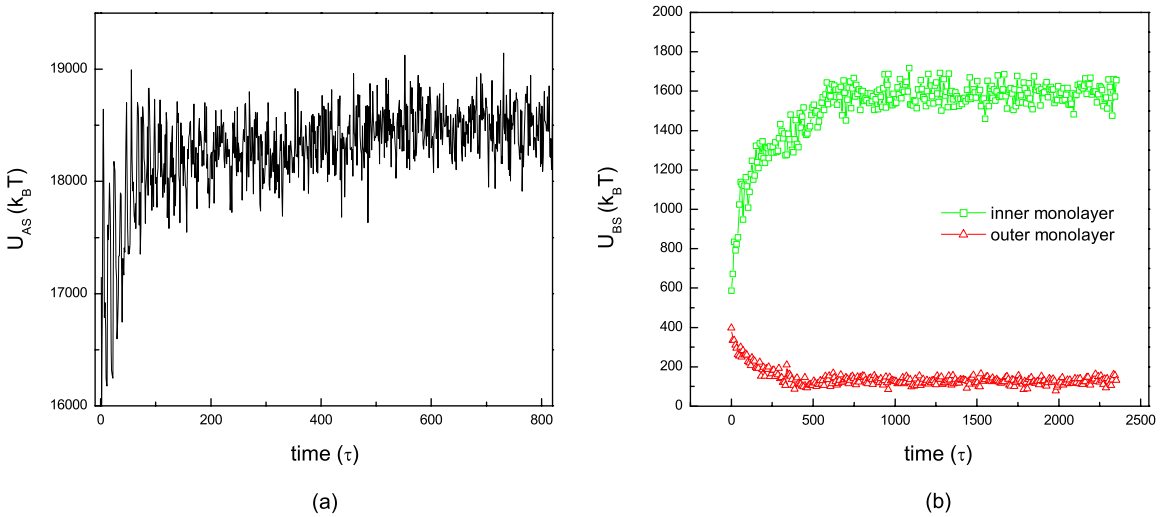

FIG. 10. (Color online) Time evolution of the interaction energy (a) between water and parent vesicle and (b) between water and domain. Φ_B=6.7%, Φ_{B1}/Φ_{B2}=3/1, R_{B1}=1.2 units of R_0, R_{B2}=0.8 units of R_0, and Π=0.78.

fluenced by the asymmetric distribution of lipids in two leaflets, domain size, area-to-volume ratio, phase-separation strength, and so forth. Only under certain conditions of these factors budding and fission could occur. Otherwise, the domain will stay in the vesicle with different curvatures [34].

C. Effects of the spontaneous curvature of the lipid and the area-to-volume ratio

The spontaneous curvature of lipid molecules plays crucial role in the shape deformation of lipid bilayer. Lipid molecules with different shapes have different spontaneous curvatures and favor different aggregated states. If the two leaflets of lipid bilayer are composed of two kinds of lipids with different spontaneous curvatures, it is always inclined to bend. It has been suggested experimentally that even small change in the head group of sterols will induce special curvature character and fission manner of the domain in GUVs [11].

In our simulation, we could adjust the effective shape of the lipid molecules by changing the radii of the head groups of the lipids. Figure 11 shows the time evolution of the interface energy of the domain (Φ_B=6.7%, Φ_{B1}/Φ_{B2}=3/1) with different radii of the head groups of lipids $B1$ and $B2$ ($\Delta R=R_{B1}-R_{B2}$). When $\Delta R \geq 0$, the domains finally realize endocytic fissions. As mentioned previously, the deformation of the domain will be slowed in the middle stages of the endocytic fission process. From Fig. 11, it is clearly shown that the spontaneous curvature of the lipid is helpful to accelerate the fission process. This promoting tendency could also be reflected from Fig. 12, which shows the mean duration of endocytic fission with different ΔR's. Herein, the fission duration is defined as the period from the beginning of the simulation to the time when the interface length of the

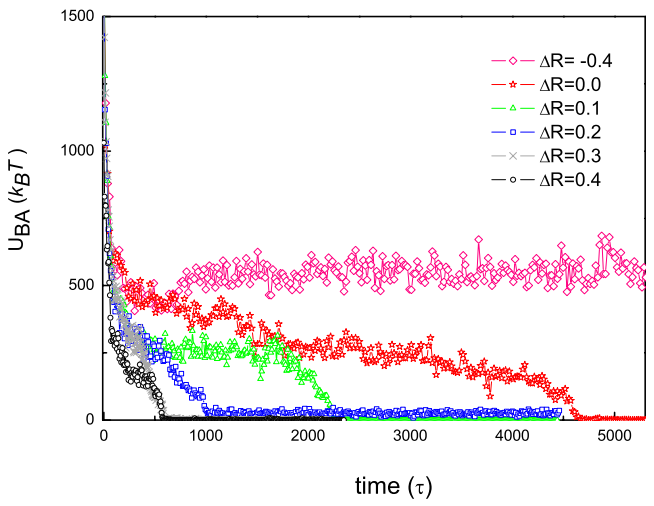

FIG. 11. (Color online) The typical time evolution of the A-B interface energy with different head radius contrasts ($\Delta R=R_{B1}-R_{B2}$) of lipids $B1$ and $B2$. The lines in figure from top to bottom correspond to ΔR=−0.4, 0.0, 0.1, 0.2, 0.3, and 0.4 units of R_0, respectively. Φ_B=6.7%, Φ_{B1}/Φ_{B2}=3/1, and Π=0.78.

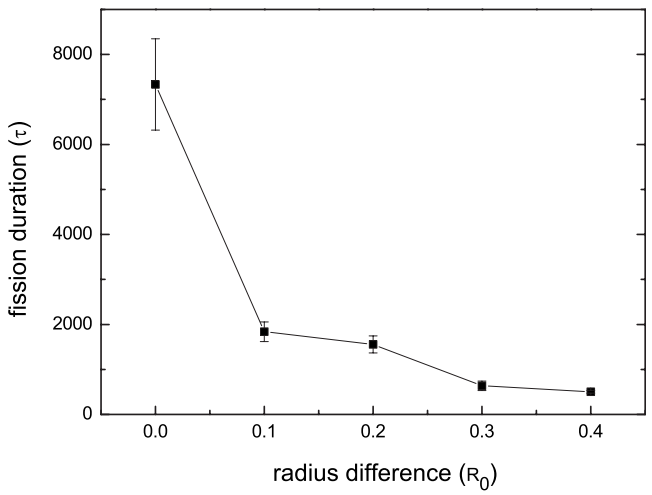

FIG. 12. Duration of endocytic fission with different head radius contrasts ($\Delta R=R_{B1}-R_{B2}$) of lipids $B1$ and $B2$. Φ_B=6.7%, Φ_{B1}/Φ_{B2}=3/1, and Π=0.78.

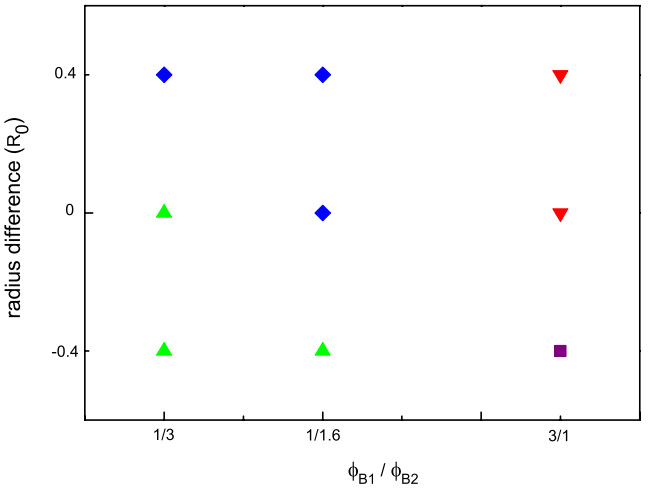

FIG. 13. (Color online) Final configurations of the domain in the vesicle with different ratios Φ_{B1}/Φ_{B2} and different head radius contrasts. The results are obtained at $t=5000$ units of τ. $\Phi_B=6.7\%$ and $\Pi=0.78$. Purple square: negative curvature; blue diamond: ellipsoidal curvature; green triangle: exocytic fission; red inverse triangle: endocytic fission.

domain becomes zero. With the decrease in ΔR, the fission duration is delayed greatly. The interval of the longest and the shortest fission processes is about 7000τ. Furthermore, if ΔR continuously decreases ($\Delta R<0$), the occurrence of the endocytic fission will become difficult. For example, when $\Delta R=-0.4$, endocytic fission is prevented and the domain keeps in the parent vesicle finally (Fig. 11). Our results indicate that the tiny changes in the head radii of the lipids have great influence on the fission process of the vesicle.

From the simulation results above, it is found that the change in the radius of the head beads of the lipids offers another possible way to control the deformation of lipid domain, which has similar influence as the change in ratio Φ_{B1}/Φ_{B2}. Figure 13 shows the possible relation between them. When $\Delta R=0$, the cases are the same as before: the domain will fission outward when $\Phi_{B1}/\Phi_{B2}=1/3$ or fission inward when $\Phi_{B1}/\Phi_{B2}=3/1$; when $\Phi_{B1}/\Phi_{B2}=1/1.6$, no fission occurs. However, the case becomes different when the effect of ΔR is included. When $\Delta R=-0.4$, the role of the spontaneous curvature of the lipid molecules is inclined to bulge the domain outward. Thus, it triggers the occurrence of exocytic fission of the domain with $\Phi_{B1}/\Phi_{B2}=1/1.6$ but impedes the invagination of the domain with $\Phi_{B1}/\Phi_{B2}=3/1$. Similarly, when $\Delta R=0.4$, exocytic fission of the domain with $\Phi_{B1}/\Phi_{B2}=1/3$ is suppressed. It is indicated that the spontaneous curvature of the lipid molecules can promote or counteract the effect of the area difference on the shape deformation of the domain.

In addition, the area-to-volume ratio is also important for the shape transformation of a vesicle. In experiment, the change in the area-to-volume ratio can be realized by adding the chemical additives or salts [12]. With the increase in the area-to-volume ratio, the vesicle becomes "floppy" and has more excess area to favor its shape transformation. This point can be demonstrated from Fig. 5. For example, for the domain of $\Phi_B=6.7\%$ and $\Phi_{B1}/\Phi_{B2}=3/1$, its final configuration is completely different under different area-to-volume ratios. When the area-to-volume ratio is large ($\Pi=0.80$ or 0.78), the domain can invaginate inward and realize the endocytic fission. With the decrease in the area-to-volume ratio ($\Pi=0.73$ or 0.71), the strong deformation of the domain is suppressed and the domain stays in the vesicle and only its curvature becomes negative.

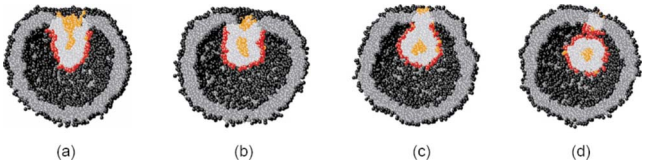

FIG. 14. (Color online) Snapshots of a possible route of endocytic fission. The cross-section images are taken at times (a) 250, (b) 375, (c) 1500, and (d) 2000 units of τ, respectively. $\Phi_B=6.7\%$, $\Phi_{B1}/\Phi_{B2}=3/1$, $R_{B1}=1.2$ units of R_0, $R_{B2}=0.8$ units of R_0, and $\Pi=0.75$.

Under the mutual effects of the area-to-volume ratio and the spontaneous curvature of lipids, another possible route of endocytic fission is observed in our simulations. When $R_{B1}=1.2$, $R_{B2}=0.8$, and $\Pi=0.75$, we observe that only a part of the domain invaginates into the parent vesicle to complete endocytic fission despite the incompatibility between two types of lipids (Fig. 14). In this case, the spontaneous curvature of the lipid molecule facilitates the invagination of the domain, but the relatively small area-to-volume ratio resists the bending of the domain.

IV. CONCLUSION

The DPD method has been carried out to study the shape deformations and fission routes of the domain, with special emphasis on the formation of the negative curvature domain and on the behavior of endocytic fission in the multicomponent vesicle. Some possible shape deformations of the domain and fission routes are obtained. We find that the asymmetric distribution of lipids in two leaflets of bilayer, the domain size, the area-to-volume ratio of the vesicle, and the spontaneous curvature of the lipid will influence the deformation direction, the evolutional routes, and the final configuration of lipid domain in the vesicle. Particularly, the negative curvature domain and endocytic fission are investigated in detail. Another possible endocytic fission route is also observed in our simulation.

ACKNOWLEDGMENTS

This work was supported by the National Basic Research Program of China Contract No. 2007CB925101 and the National Natural Science Foundation of China Contracts No. 10629401 and No. 20674037.

[1] O. G. Mouritsen, *Life—As a Matter of Fat* (Springer-Verlag, Berlin, 2005).
[2] K. Simons and D. Toomre, Nat. Rev. Mol. Cell Biol. **1**, 31 (2000).
[3] A. S. Shaw, Nat. Rev. Immun. **7**, 1139 (2006).
[4] S. L. Veatch and S. L. Keller, Phys. Rev. Lett. **89**, 268101 (2002).
[5] M. Yanagisawa, M. Imai, and T. Taniguchi, Phys. Rev. Lett. **100**, 148102 (2008).
[6] H. T. McMahon and J. L. Gallop, Nature (London) **438**, 590 (2005).
[7] T. Baumgart, S. T. Hess, and W. W. Webb, Nature (London) **425**, 821 (2003).
[8] J. Zimmerberg and L. V. Chernomordik, Science **310**, 1626 (2005).
[9] T. Tanaka, R. Sano, Y. Yamashita, and M. Yamazaki, Langmuir **20**, 9526 (2004).
[10] G. Staneva, M. Seigneuret, K. Koumanov, G. Trugnan, and M. I. Angelova, Chem. Phys. Lipids **136**, 55 (2005).
[11] K. Bacia, P. Schwille, and T. Kurzchalia, Proc. Natl. Acad. Sci. U.S.A. **102**, 3272 (2005).
[12] T. Hamada, Y. Miura, K. Ishii *et al.*, J. Phys. Chem. B **111**, 10853 (2007).
[13] M. V. Gudheti, M. Mlodzianoski, and S. T. Hess, Biophys. J. **93**, 2011 (2007).
[14] H. Matsuo, J. Chevallier, N. Mayran *et al.*, Science **303**, 531 (2004).
[15] A. J. Markvoort, A. F. Smeijers, K. Pieterse, R. A. van Santen, and P. A. J. Hilbers, J. Phys. Chem. B **111**, 5719 (2007).
[16] M. Laradji and P. B. Sunil Kumar, Phys. Rev. Lett. **93**, 198105 (2004).
[17] S. Yamamoto and S. Hyodo, J. Chem. Phys. **118**, 7937 (2003).
[18] Y. E. Maruvka and N. M. Shnerb, Phys. Rev. E **73**, 011903 (2006).
[19] W. Shinoda, N. Namiki, and S. Okazaki, J. Chem. Phys. **106**, 5731 (1997).
[20] B. J. Reynwar, G. Illya, V. A. Harmandaris, M. M. Muller, K. Kremer, and M. Deserno, Nature (London) **447**, 461 (2007).
[21] I. R. Cooke, K. Kremer, and M. Deserno, Phys. Rev. E **72**, 011506 (2005).
[22] J. C. Shillcock and R. Lipowsky, J. Chem. Phys. **117**, 5048 (2002).
[23] A. Grafmuller, J. Shillcock, and R. Lipowsky, Phys. Rev. Lett. **98**, 218101 (2007).
[24] D. W. Li and X. Y. Liu, J. Chem. Phys. **122**, 174909 (2005).
[25] K. Yang and Y. Q. Ma, J. Phys. Chem. B **113**, 1048 (2009).
[26] B. B. Hong, F. Qiu, H. D. Zhang, and Y. L. Yang, J. Phys. Chem. B **111**, 5837 (2007).
[27] R. D. Groot and K. L. Rabone, Biophys. J. **81**, 725 (2001).
[28] K. A. Smith and W. E. Uspal, J. Chem. Phys. **126**, 075102 (2007).
[29] D. W. Li, X. Y. Liu, and Y. P. Feng, J. Phys. Chem. B **108**, 11206 (2004).
[30] P. J. Hoogerbrugge and J. M. V. A. Koelman, EPL **19**, 155 (1992).
[31] P. Español and P. Warren, EPL **30**, 191 (1995).
[32] I. Vattulainen, M. Karttunen, G. Besold, and J. M. Polson, J. Chem. Phys. **116**, 3967 (2002).
[33] M. Laradji and P. B. Sunil Kumar, Phys. Rev. E **73**, 040901(R) (2006).
[34] T. Taniguchi, Phys. Rev. Lett. **76**, 4444 (1996).
[35] J. Liu and J. C. Conboy, Biophys. J. **89**, 2522 (2005).
[36] P. F. Devaux and R. Morris, Traffic (Oxford, U. K.) **5**, 241 (2004).
[37] Y. Inaoka and M. Yamazaki, Langmuir **23**, 720 (2007).
[38] U. Seifert, Adv. Phys. **46**, 13 (1997).
[39] L. Miao, U. Seifert, M. Wortis, and H. G. Dobereiner, Phys. Rev. E **49**, 5389 (1994).
[40] S. Baoukina, L. Monticelli, H. J. Risselada, S. J. Marrink, and D. P. Tieleman, Proc. Natl. Acad. Sci. U.S.A. **105**, 10803 (2008).